Numerical Investigation of Floating Pile Performance near Excavation Activities in Soft Clay Using 3D FEM

[1]Abhay Singh*, [2]Er. Nitin Verma, [3]Dr. Naveet Himanshu, [4]Chandan Kumar
[1]Student, [2]Assistant Professor, [3]Assistant Professor
[1, 2, 3] Affiliation Address: Chandigarh University, NH, Chandigarh State, Punjab-140413
[4]Affiliation Address: GNA University Phagwara, Punjab
[1]Email: abhayrana807@gmail.com, [2]Email: nitin.e1939@cumail.in
[3]Email: navneet.e12108@cumail.in, [4]Email: chandan.kumar@gnauniversity.edu.in
*Corresponding Email: abhayrana807@gmail.com

Abstract
Deep underground infrastructure excavation in the fast urbanizing cities are being progressively carried out near the current pile foundation, which is a cause of concern due to the excavation caused ground movement and its effect on the performance of piles in soft clay. Excavation stress redistribution may result in piles settlement, lateral deflection, and an increase in bending moment, which may pose a threat to the structural safety. The study will deal with this issue by exploring numerically the behavior of a single floating pile in the presence of excavations at various depths and conditions of construction. A hypoplastic constitutive model was used to formulate a 3D coupled consolidation finite element model to model realistically the nonlinear behavior of clay and the small strain stiffness. Three excavation depth ratios (0.67/Lp, 1.00/Lp, 1.33) and different fixing of the pile head, as well as working loads at the factors of safety of 3 and 1.5, were the parameters of analysis. The mathematical model was tested on centrifuge test results found in the literature. The findings show that the excavation depth is the most important factor that governs the response of the piles. Topical pile settlements of 24 mm, 38 mm, and 50 mm on He/Lp ratios of 0.67, 1.00 and 1.33, respectively, and bending moment under fixed head conditions of close to 60% of the moment capacity of the pile was achieved thus placing the importance on excavation design around piled foundations.

Keyword: Finite component analysis, Digging depths, Single pile, Pile-soil interaction.
How to cite this article: Singh A, Verma N, Himanshu N, Kumar C. Numerical Investigation of Floating Pile Performance near Excavation Activities in Soft Clay Using 3D FEM. Int J Drug Deliv Technol. 2026;16(59s): 1737-1746. DOI: 10.25258/ijddt.16.59s.198
Source of support: Nil
Conflict of interest: None

1. Introduction

In geotechnical engineering, it is commonly understood that loads from the superstructure are transmitted to the ground through pile foundations. Around the pile shafts and beneath the pile tips, stress concentration areas develop—often known as stress bulbs—where the effective stress is significantly higher than the surrounding ground. When excavation occurs nearby, this stress regime alters, triggering ground movements as the soil adjusts to the new stress distribution. In modern urban environments, subsurface transport infrastructure, including metro tunnels, underground stations, and multi-level parking basements, plays a key role in managing congestion in high-density cities such as Shanghai and Hong Kong. Often, these underground structures are constructed in close proximity to pre-existing piled foundations, posing serious challenges for geotechnical engineers in ensuring foundation stability under excavation-induced stress relief (Leung et al., 2000; Ong et al., 2006).

Field observations and model experiments have shown that excavations in soft soils can induce significant lateral displacements, which negatively affect nearby piles by increasing bending moments and lateral deflections. Centrifuge model tests in soft kaolin clay demonstrated that pile head fixity and the distance between the excavation wall and the piles significantly influenced the structural response, including bending and deformation patterns (Ong et al., 2006). These studies confirmed that piles subjected to initial vertical loading before excavation respond differently than those that are unloaded, as preloading increases the effective stress in the surrounding soil, modifying subsequent pile-soil interactions. In dense dry sands, additional centrifuge studies were carried out to understand pile behavior under adjacent unbraced excavations. It was observed that both the pile head condition and the separation between the pile and excavation wall control the magnitude of lateral deflections and internal bending moments (Leung et al., 2003; Leung et al., 2006).

Ng et al. (2017) extended this work by conducting in-flight experiments on single piles subjected to multi-prop deep excavations, where lateral movement constraints affected the pile behavior both above and below the ground surface. Results showed that pile head restraint considerably impacts the bending moment profile and that under certain configurations; these moments could exceed the pile's ultimate bending resistance. Finite element methods (FEM) have proven effective for simulating pile behavior under excavation-induced ground movements. Shakeel and Ng (2018) developed a 3D coupled consolidation model to study a floating pile group positioned near a deep excavation in soft clay. Their study found that maximum settlement occurred when the pile group was located at excavation depth and about 0.75 times the excavation depth away from the wall. Moreover, tilting effects were noted to diminish as the pile group moved closer to the retaining structure.

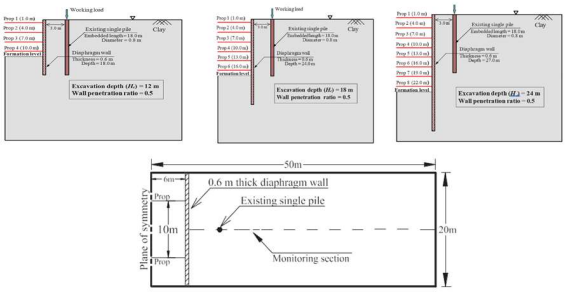

Figure 1: Numerical simulation setup showing elevation and plan views for different He/Lp ratios (0.67, 1.00, and 1.33)

In a numerical investigation, Li et al. (2014) used the "Modified Cam-Clay (MCC)" model to assess pile deflection, bending moments, and lateral soil pressures under various excavation and pile configurations. Their results showed that pile stiffness, axial loading, wall stiffness, and distance to excavation all significantly influence behavior. Zhang et al. (2018), employing the Hardening Small Strain (HSS) model, further supported these findings by demonstrating that even small strain levels could result in highly nonlinear soil responses when influenced by excavation activity. These nonlinear stress-strain relationships are crucial in understanding and modeling excavation-induced ground movement and its impact on nearby foundations.

Korff et al. (2016) proposed an analytical framework to connect vertical soil displacements to axial deformations in piles subjected to excavation. Their nonlinear load-transfer model considered axial stress, relative movement, and stiffness variations. The study concluded that pile settlement, especially in high shaft-friction conditions, depends heavily on the self-weight-to-capacity ratio and the relative stiffness between pile and surrounding soil. This research systematically examines how different excavation depths affect the loading behavior of a single floating pile during various construction phases. The study also evaluates the influence of pile head boundary conditions and working loads on pile performance. Key response parameters including settlement patterns, axial load transfer mechanisms, lateral displacements, bending moment distributions, effective stress changes, and excess pore water pressure development are thoroughly analyzed throughout the excavation process. Here are some research objectives of the study follows as:

I. To examine the influence of nearby deep excavation activities on the mechanical response of a single floating pile embedded in soft clay.
II. To evaluate the effects of different excavation depth ratios (He/Lp) on pile settlement, lateral displacement, axial load transfer, and bending moment distribution.
III. To assess the role of pile head boundary conditions (free, pinned, and fixed) on pile behavior during staged excavation.
IV. To examine the impact of varying working loads corresponding to different factors of safety on pile performance.
V. To develop 3D coupled consolidation FEM using an advanced hypoplastic constitutive law capable of capturing nonlinear and small-strain soil behavior.
VI. To validate the numerical model against published centrifuge test data and assess its reliability.
VII. To provide insights and design-oriented recommendations for the safe construction of deep excavations in close proximity to existing pile foundations in soft clay soils.

2. Literature Review

In the recent past, there have been numerous research activities particularly on the soil structure interaction issues related to tunnelling, excavation and foundation works in soft ground through the application of sophisticated numerical and field based methods. Soomro et al., (2025) established that close tunnel excavation influences greatly on the pile-supported embankments when it is on soft clay, and the patterns of deformation are highly dependent on the alignment of the tunnels and their level of consolidation. On the same note, Xu et al., (2025) also pointed out the weakness of low-strength buildings located in soft alluvial deposits during the subway excavation that is large-scale in nature, and the rationale of staged excavation, monitoring and integrated systems of underpinning. Huang et al., (2025) also demonstrated that excavation width is a

very important factor in regulating the movement of the walls and ground settlement in soft clay where a wider excavation results in decreased constraint in the passive zone and increased deformation. He et al., (2024) also supplemented these results by showing the coupled effect of soil-blocking and water-blocking of current pile foundations which occur during pre-excavation dewatering and that the distance and groundwater conditions play a critical role in settlement mechanisms.

Table 1: Comparison of literature review

Author (Year)	Study Focus	Methodology / Model	Soil / Site Condition	Key Parameters Investigated	Major Findings
Soomro et al. (2025)	Effect of adjacent tunnelling on pile-supported embankment	3D coupled hydro-mechanical numerical modeling; hypoplastic model with intergranular strain	Soft clay	Tunnel alignment (S, T, B), consolidation state	Maximum settlements of 0.49%, 0.20%, and 0.45%; consolidation reduced settlement and bending moment (max 142 kNm unconsolidated)
Xu et al. (2025)	Response of low-strength buildings to nearby subway excavation	Field monitoring + numerical analysis + underpinning	Soft alluvial clay (Yangtze River area)	Excavation stages, underpinning system	Early-stage settlement reached ~28% of final values; underpinning effectively reduced post-excavation settlement
Huang et al. (2025)	Influence of excavation width on deformation	2D numerical simulations (40 models)	Shanghai soft clay	Excavation width, depth	Wall displacement and settlement increase with width but at decreasing rate due to reduced passive zone constraint
He et al. (2024)	Effect of dewatering near existing piles	Numerical simulation + field measurements	Soft soil with high groundwater	Distance between pit and piles (D)	Soil-blocking dominant for $D \leq 40$ m; water-blocking increases settlement when $D > 40$ m
Li et al. (2023)	Passive pile and pile-group response to excavation	Mindlin solution + Pasternak model + FDM	Elastic soil idealization	Excavation-induced lateral stress, pile shielding	Proposed two-step method accurately predicts pile and pile-group deflect

					ions
Wang et al. (2023)	Building–pile–excavation interaction	3D numerical modeling	Urban soft soil	Building height, distance (D), orientation (θ)	Taller buildings and smaller D significantly increase pile bending moments and settlements
Yin et al. (2023)	Optimization of foundation pit support system	Numerical simulation + field validation	Soft soil	Support type, pile depth, beam size	PARB system improved support efficiency by ~30% compared to PAB
Negesa (2022)	Consolidation settlement of culvert on soft clay	FEM (GeoStudio/SigmaW) + field monitoring	Soft compressible clay	Wick drain spacing, fill thickness	Numerical and field results matched well (max deviation 0.0305 m)
Zhuang et al. (2022)	Uplift behavior of HSCM piles	3D FEM analysis	Marine soft clay	Strength ratio (Cref/su), failure mode	Uplift capacity increases with strength ratio; empirical design formula proposed
Lee et al. (2022)	Excavation near operational railway	3D FEM + construction monitoring	Gravel layer	Excavation sequence, support piles	Numerical predictions agreed well with monitoring; method deemed safe
Fall et al. (2021)	Effect of pile driving on adjacent piles	3D ALE FEM with element deletion	Soft ground	Pile spacing, pile shape	Significant induced bending and axial forces; tapering reduces adverse effects

Other researchers considered pile behavior and support systems under excavation-induced loading. Li et al., (2023) developed a two-step analytical solution to predict passive pile and pile-group deformation, accounting for shielding effects between piles. Wang et al., (2023) determined the quantitative effects of building height, distance, and orientation on the adjacent deep foundation pit piles' internal forces. Yin et al., (2023) verified that improved support systems, such as the pile-anchor-ribbed-beam configuration, can greatly increase excavation stability in soft soils. Long-term consolidation behavior and new innovative pile solutions in soft clay were discussed by Negesa (2022) and Zhuang et al., (2022). Three-dimensional numerical modeling was stressed by Lee et al., (2022) as well as construction effects on adjacent piles and infrastructure safety by Fall et al., (2021). Together these studies prove that excavation geometry; soil constitutive behavior; groundwater conditions; and foundation type all control deformation together with structural safety in a soft ground environment.

3. Study of 3D Coupled Consolidation

3D coupled consolidation numerical parametric research was conducted to compare the impacts of different excavation depths on piled foundations on soft clay. The investigation focused on three different pile shaft heights (He/Lp): He/Lp = 0.67 at the soil surface, He/Lp = 1.00 at the pile toe, and

He/Lp = 1.33 below the pile. These measured 12 meters, 18 meters, and 24 meters in length, with a diameter of 0.8 meters and a pile length (Lp) of 18 meters. It was originally believed that the pile was a cylinder of concrete capable of withstanding a bending moment of 800 kNm.

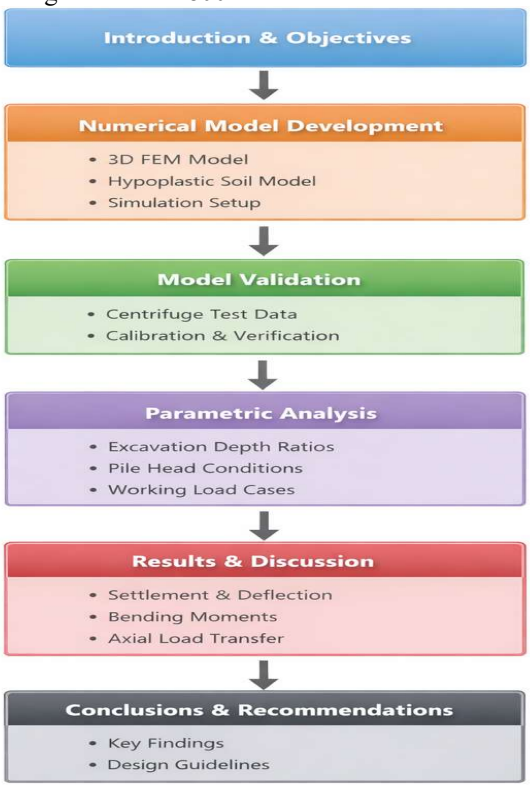

Figure 2: Flowchart of suggested work

A 0.6 m thick diaphragm wall, with a 0.5 m wall-to-excavation depth and a 3 m vertical spacing, supported the excavation, and 10 m horizontal spacing over 2 m tall props were placed and modelled as a soft element (axial rigidity: 81 x 10 3 kNm). The pile wall offset's length was fixed at 3.0 meters. A number of working loads by using a factor of safety of 3.0 and 1.5 were used to compare the available pile head fixity conditions such as free, pinned, and fixed in order to analyze the responses of piles. And finally, four post-analyzed simulations were also created using the free-field conditions to determine the settlement profiles and ultimate axial pile capacity. Sums of 16 simulations were carried out. Due to symmetry, only half of the 12-meter-deep excavation would be modeled and the monitoring would be along the centerline of the excavation.

3.1 Numerical Mesh Configuration and Boundary Constraints

The finite element modeling tool that is to be used in this research is Abaqus (2010). The mesh size will be 50 m x 20 m x 40 m (in x-axis, y-axis, and z-axis respectively). The mesh size will therefore be variable with respect to each numerical run. The earth, pile, diaphragm wall are modeled by eight node hexahedral brick elements whereas the props have been modeled by two node truss element. A 17-day simulation with He/Lp of 0.67, 25-day simulation with He/Lp of 1.00 and a 35-day simulation with He/Lp of 1.33 were performed.

The pins support the base ofthe mesh and the rollers support its sides that are vertical. With this, all base directions and motions normal to the vertical bounds are limited. People assume that the underground water table lies on the surface of the ground. A hydrostatic distribution of pore water pressure is first suggested. Access for free drainage is granted at the edge of the mesh construction site. The points where wall-soil and pile-soil meet are modeled using duplicate nodes in which they are assigned a zero thickness. The Coulomb law of friction defining the interface requires as input parameters the limiting displacement (6) and the interface friction coefficient (6). It is thought that when there is a limiting shear displacement of 5 mm, where 0—the normal effective stress between two contact surfaces—can be obtained using typical values as 0.35 and every analysis using the number 0.35, full mobilization of the interface friction equal to muscle times less than or equal to p occurs (Lee and Ng, 2004). Sections of dirt inside the excavation region will be turned off to replicate the excavation process. The truss elements providing the props will be brought to play in the meanwhile.

3.2 Constitutive Modeling and FE Simulation Input Parameters

With regard to simulating the nonlinearity of granular materials at medium and large strain deformations due to monotonic loading, the fundamental hypoplastic model is unique because of this (M a Five fundamental parameters N as well as Camb is the slope of the isotropic unloading line on the same plot, Camb is the critical state friction angle, and r controls the large-strain shear modulus. Camb is also the plane of ln(1 + e) vs lnp', where e is the void ratio and p' is the mean effective stress. To improve the model's functionality, Niemunis and Herle (2005) suggested an intergranular strain concept and the additional five parameters namely R (elastic range), βr and χ (stiffness degradation rate), and mT and mR (initial shear modulus adjustment) were introduced. Continuing with the use of the model, the hypoplastic clay model (Gudehus et al., 2008) that considers the effect of small-strain stiffness has been coded in Abaqus (2010) by a user-defined subroutine. The step 9, Soils, in Abaqus is used to perform analysis of partially or fully saturated fluid flow in porous media using the effective stress principle, where the total stress tensor (σij) combines effective stress (σ'ij) and

pore fluid pressure (p) as σij = σ'ij + pδij (where δij is the Kronecker delta). This framework provides a comprehensive approach for modeling complex soil behavior under various loading conditions.

Table 2: Summary of Numerical solutions

Variable	Excavation depth (m)	Diaphragm wall depth (m)	Pile head condition	Working load (kN)	Objective
Excavation effect on pile					
Excavation & wall depth	12.0	18.0	Free	720	Effects of excavation depths
	18.0	24.0		720	
	24.0	36.0		720	
Pile head condition	12.0	18.0	Pinned & fixed	720	Effects of pile head conditions
	18.0	24.0	Pinned & fixed	720	
	24.0	36.0	Pinned & fixed	720	
Working load	12.0	18.0	Free	1440	Effects of different working loads
	18.0	24.0		1440	
	24.0	36.0		1440	
Excavation in greenfield condition					
Excavation & wall depth	12.0	18.0	N.A.	N.A.	To compute ground and subsurface settlement due to excavation in free-field condition
	18.0	24.0			
	24.0	36.0			

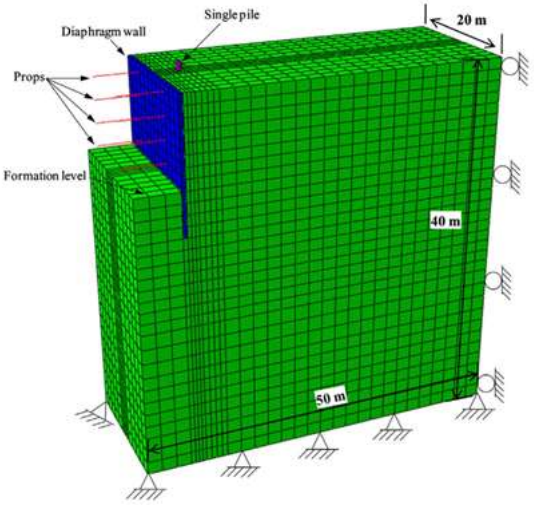

Figure 3: Boundary conditions and finite element mesh of a standard numerical analysis with a height-to-length ratio (He/Lp) of 0.67

Table 3: Parametric study uses model parameters of the kaolin clay

Description	Parameter
Effective angle of shearing resistance at critical state, φ′	22°
Parameter controlling the slope of the isotropic normal compression line in ln(1 + e) versus ln p plane, λ*	0.11
Parameter controlling the slope of the isotropic normal compression line in the ln(1 + e) versus ln p plane, κ*	0.026
Parameter controlling the position of the isotropic normal compression line in the ln(1 + e) – ln p plane, N	1.36
Parameter controlling the shear stiffness at medium to large strain levels, r	0.65
Parameter controlling initial shear modulus upon 180° strain path reversal, m_p	14
Parameter controlling initial shear modulus upon 90° strain path reversal, m_t	11
Size of elastic range, R	1×10^{-5}
Parameter controlling the rate of degradation of the stiffness with strain, β_r	0.1
Parameter controlling degradation rate of stiffness with strain, χ	0.7
Initial void ratio, e_0	1.05
Dry density (kg/m³)	1136
Coefficient of permeability, k (m/s)	1×10^{-9}

3.3 Numerical Modelling Procedure

The (He/Lp) value 0.67 was utilized as the basis for the computational model. Boundary conditions and the starting state of effective stress under the assumption of vertical ground pressure were used in the simulation, coefficient keeps to 0.63. Then the model was filled in with a single pile using the so-called wished-in-place method with brick components. After this, a working load (which was calculated by conducting numerical pile load testing previously) was used on the pile. This generated overflowing pore pressure which was not artificially relieved. Then, the diaphragm wall items in the model were switched on. Diggings were also emulated, and this can be categorized as a multi-propped set up. The initial excavation phase extended to 3 meters and the first level of prop was fixed at 1m below the ground level. This was done piecemeal as the pieces are excavated and support installed until the maximum excavation depth of 12 meters is reached.

3.4 Numerical Model Centrifuge Test Verification

The correctness of the numerical model's formulation was ensured by using centrifuge test data released by Ong et al. (2006). It was carried out using the hypoplastic clay model's parameters, which had previously been adjusted based on the outcomes of laboratory tests. The centrifuge test was back-analyzed, allowing for a direct comparison between the numerical prediction and the actual behavior that was seen.

- **Centrifuge Test Setup and Methodology**

To find out how a single pile will react to a nearby excavation in Kaolin clay, Ong et al. (2006) conducted an experiment using a centrifuge test with a centrifugal acceleration of 50g. This was set at a bored pile of concrete with 600 mm diameter which was embedded to a depth of 12.5 m (at prototype) and was placed side by side a diaphragm wall made of aluminium of 3 mm thickness. The wall would have a flexure stiffness that is equal to those of an FSP-IIA steel sheet pile. The draining of a $ZnCl_2$ solution into a controlled draining to the same depth (1.2 m) was used to replicate a latex membrane in flight. The model was built in a strongbox that measured 540 mm by 200 mm by 470 mm, or 27 m by 10 m by 23.5 m in that instance. A 120 mm thick layer of sandy sediment that served as a drainage border was covered with the Kaolin clay slurry, which had an initial water content of 120%. Following the installation of the wall and pile at 1g, a latex bag filled with $ZnCl_2$ solution partially replaced the clay, and the model was centrifuged to reconsolidate.

- **Back-Analysis Modelling Technique**

Finite element mesh in the back-analysis was made to simulate the actual dimension utilized in the centrifuge model. The displacement of the mesh end boundaries was against the surface restricted. The soil mass and structural weights were represented using eight-node brick elements, while the pile was modeled using four-node shell elements. The bedrock under this layer of sands was assumed to be modelled under Mohr-Coulomb soil model. Some important properties of the sand like friction angle 43 deg, unit weight 15.78kN/m^3, and dilation angle 12 deg were taken over by the past studies. The cyclic modelling process involved the determination of initial stress state of K0 = 0.5 at 1g, energizing of the pile and wall, placing the solution pressure on the pile due to hydrostatic pressure 0.5 in $ZnCl_2$ solution, test setting the 50g gravitational loading and the lastly, the excavating process which was simulated through the removal of the $ZnCl_2$ pressure.

4. Numerical and Experimental Results Evaluation

Comparison between simulation results with those of centrifuge tests was done to assess model performance. Surface settlement records were recorded at horizontal distance of 0.2 pile diameter (averagely) away of the geographical centre of the piles. These settlements as well as the horizontal distances were standardized against the final depth of excavations (He). The calculated settlement trough was close to the observed data, and had a shape of a spandrel, which is typical in unsupported excavations. The maximum settlement of 0.67He (or about 0.8 m) was observed 0.67He (or about 0.8 m) away the wall, having a normalized value of settlement along (s/He) of 8.0%. The analytical solution also revealed that the pile moved towards the excavation through stress release in the process of excavation.

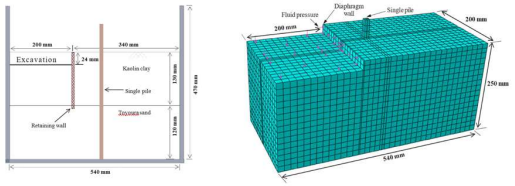

Figure 4: According to Ong et al. (2006), the centrifuge test specifics were as follows: (a) Model setup elevation view; (b) matching finite element mesh for numerical back-analysis

4.1 Analysis and Interpretation of Simulation Results

The ground surface settlements caused by excavation behind retaining wall under free-field condition are shown in figure below under three different conditions, namely, He/Lp = 0.67, 1.00 and 1.33. To be explicit, settlement profiles are presented at excavation end.

The findings point toward the fact that in all instances, the spandrel-like character of a settlement pattern was created. The greatest settlement was found around 2.8 meters behind the wall, and it gradually diminished as one moved further away (as shown by a negative slope). In order to examine the impact of the excavation on the pile, a clear 3 m gap between the pile and the wall was obtained for further investigation.

Both the lateral length of the settlement trough and the intensity of the maximum settlement increased with increasing excavation depth. Specifically, it was observed that the highest settlements were 24 mm (He/Lp = 0.67), 38 mm (He/Lp = 1.00), and 50 mm (He/Lp = 1.33).

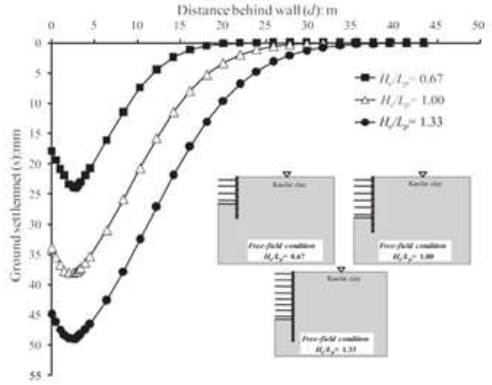

Figure 5: Following excavation, ground surface settlements were noted in all three instances under free-field circumstances (i.e., He/Lp = 0.67, 1.00, and 1.33).

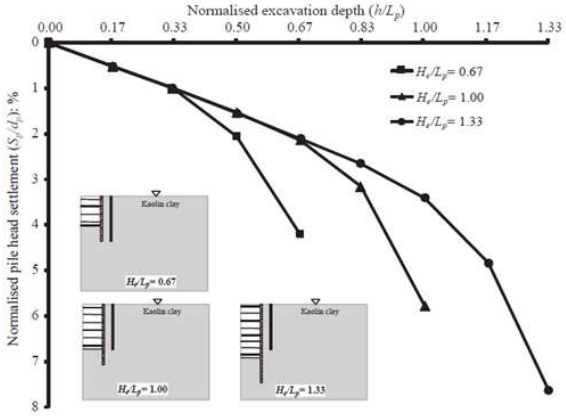

Figure 6: Ground surface settlements during excavation, normalized

The ground surface settlements caused by excavation behind retaining wall under free-field condition are shown in figure below under three different conditions, namely, He/Lp = 0.67, 1.00 and 1.33. To be explicit, settlement profiles are presented at excavation end.

The findings point toward the fact that in all instances, the spandrel-like character of a settlement pattern was created. The greatest settlement was found around 2.8 meters behind the wall, and it gradually diminished as one moved further away (as shown by a negative slope). In order to examine the impact of the excavation on the pile, a clear 3 m gap between the pile and the wall was obtained for further investigation.

Both the lateral length of the settlement trough and the intensity of the maximum settlement increased with increasing excavation depth. Specifically, it was observed that the highest settlements were 24 mm (He/Lp = 0.67), 38 mm (He/Lp = 1.00), and 50 mm (He/Lp = 1.33).

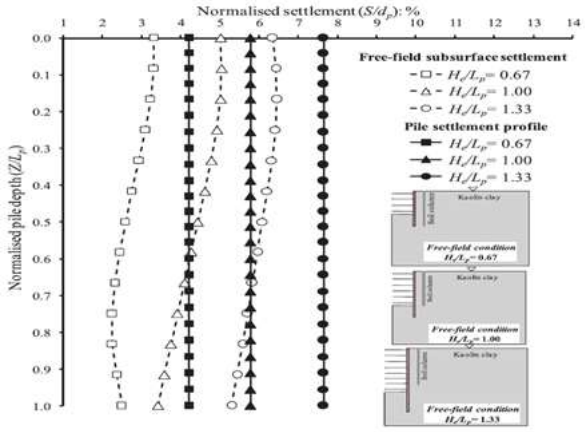

Figure 7: Settlement behavior of piles and surrounding soil was evaluated at embedment ratios He/Lp = 0.67, 1.00, and 1.33

5. Discussion

The analytical model of the floating piles performance that was subject to the investigation on the performance of the piles in the vicinity of excavations in soft clay provided important results. The test revealed the fact that the maximum as excavation depth grew, pile settling increased as well, taking on considerable values at various excavation depths. To be precise, under certain excavation depth ratio the maximum settlement is found to be 24mm, under another, the maximum settlement has a value of 38mm and under the most extreme excavation scenario maximum settlement is found as 50mm. This implies a direct relationship between excavation depths with the piles response. Also, the outcome was the fact that the piles deflected towards the excavation as a result of the stress being released hence a typical settlement pattern. The spacing between the pile and the excavation wall was also determined to have a big impact on the pile's behavior, whereby a certain distance was taken as a reference in doing further analysis. The results supported the relevance of the retaining wall's

embedded depth because the deepest settlement was associated with the greatest excavation condition.

6. Conclusion

This paper presents a detailed numerical evaluation of the behavior of one floating pile in the presence of deep excavations in soft clay, showing the complex interaction processes between soil and structure caused by stress relief created by excavations. Results provided are a clear indication that the depth of excavation is the most significant parameter that has a controlling effect on the pile response. With a growing depth of the excavation, the settlement of the piles, their lateral displacement, and bending moments also grow to significant values, and He/Lp = 1.33 scenario has resulted in the most critical behavior. The highest pile settlement was about 50 mm, and the bending moments under the fixed-head conditions were nearly 60% of the bending capacity of the pile, which means that there is a risk of structural safety being at risk unless the effect of excavations is sufficiently taken into account. Other factors that were identified to affect the performance of piles include pile head restraint and level of working load, but this was seen to have secondary effects as compared to the excavation depth. The paper validates that 3D coupled consolidation analysis that is used along with sophisticated hypoplastic soil modeling can realistically simulate excavation-pile interaction in soft clays.

Future studies should aim at extending this framework to pile groups and piled raft systems in order to reflect more realistic foundation conditions. The influence of different soil stratigraphy, anisotropy, and time-dependent consolidation should also be addressed. The incorporation of field monitoring data and the study of post-excavation long-term behavior would enhance model validation and contribute to the formulation of safer and more robust foundation design guidelines in the vicinity of deep excavations.

References

1. Fall, M., Gao, Z., & Ndiaye, B. C. (2021). Driven pile effects on nearby cylindrical and semi-tapered pile in sandy clay. *Applied Sciences*, *11*(7), 2919.
2. Franza, A., & Marshall, A. M. (2017). Centrifuge modelling of tunnelling beneath axially loaded displacement and non-displacement piles in sand. In T. L. Brandon & R. J. Valentine (Eds.), *Proc. Geotech. Front. 2017. GSP 277 Transp. Facil. Struct. site Investig.* (pp. 576–586). Orlando, Florida.
3. Franza, A., & Marshall, A. M. (2018). Centrifuge modeling study of the response of piled structures to tunneling. *Journal of Geotechnical and Geoenvironmental Engineering, 144*(4), 04017109. https://doi.org/10.1061/(ASCE)GT.1943-5606.0001751
4. Goh, A. T. C., Wong, K. S., Teh, C. I., & Wen, D. (2003). Pile response adjacent to braced excavation. *Journal of Geotechnical and Geoenvironmental Engineering, 129*(4), 383–386.
5. Gudehus, G., Amorosi, A., Gens, A., Herle, I., Kolymbas, D., Mašín, D., Wood, M., Nova, R., Niemunis, A., Pastor, M., Tamagnini, C., & Viggiani, G. (2008). The soilmodels.info project. *International Journal for Numerical and Analytical Methods in Geomechanics, 32*(12), 1571–1572.
6. He, D., Zeng, C., Xu, C., Xue, X., Zhao, Y., Han, L., & Sun, H. (2024). Barrier Effect of Existing Building Pile on the Responses of Groundwater and Soil During Foundation Pit Dewatering. *Water (20734441)*, *16*(20).
7. Hsiung, B. C. B. (2009). A case study on the behaviour of a deep excavation in sand. *Computers and Geotechnics, 36*(4), 665–675.
8. Huang, P., Dang, K., Shi, H., Yang, K., & Wu, J. (2024). Influence and mechanism of the excavation width on excavation deformations in shanghai soft clay. *Buildings*, *14*(5), 1450.
9. Korff, M., Mair, R. J., & Van Tol, F. A. F. (2016). Pile-soil interaction and settlement effects induced by deep excavations. *Journal of Geotechnical and Geoenvironmental Engineering, 142*(8), 04016034.
10. Lee, C. J., & Chiang, K. H. (2007). Responses of single piles to tunneling-induced soil movements in sandy ground. *Canadian Geotechnical Journal, 44*(11), 1224–1241. https://doi.org/10.1139/T07-050
11. Lee, C. J., & Ng, C. W. W. (2004). Development of downdrag on piles and pile groups in consolidating soil. *Journal of Geotechnical and Geoenvironmental Engineering, 130*(2), 905–914.
12. Lee, Y. L., Hsu, W. K., Hsieh, P. W., Ma, C. H., Lin, M. Y., & Lee, C. M. (2022). Mechanical Behavior Analysis of Excavation and Retaining Piles in Gravel Formation along Adjacent Railways: A Comparative 3D FEM Study with Monitoring Data. *Applied Sciences*, *13*(1), 397.
13. Leung, C. F., Chow, Y. K., & Shen, R. F. (2000). Behavior of pile subject to excavation-induced soil movement. *Journal of Geotechnical and Geoenvironmental Engineering, 126*(11), 947–954.
14. Leung, C. F., Lim, J. K., Shen, R. F., & Chow, Y. K. (2003). Behavior of pile groups subject to excavation-induced soil movement. *Journal of*

Geotechnical and Geoenvironmental Engineering, 129(1), 58–65.

15. Leung, C. F., Ong, D. E. L., Shen, R. F., & Chow, Y. K. (2006). Pile behavior due to excavation-induced soil movement in clay II: Collapsed wall. *Journal of Geotechnical and Geoenvironmental Engineering, 132*(1), 45–53.
16. Li, L., Hu, X. X., Dong, G. H., & Liu, J. (2014). Three-dimensional numerical analyses of pile response due to braced excavation-induced lateral soil movement. *Applied Mechanics and Materials, 580–583*, 524–531.
17. Li, T., Yang, M., & Chen, X. (2023). A Simplified Analytical Method for the Deformation of Pile Foundations Induced by Adjacent Excavation in Soft Clay. *Buildings*, *13*(8), 1919.
18. Liyanapathirana, D., & Nishanthan, R. (2016). Influence of deep excavation induced ground movements on adjacent piles. *Tunnelling and Underground Space Technology, 52*, 168–181.
19. Mašín, D. (2009). 3D modeling of an NATM tunnel in high K0 clay using two different constitutive models. *Journal of Geotechnical and Geoenvironmental Engineering, 135*(9), 1326–1335.
20. Mašín, D., & Herle, I. (2005). State boundary surface of a hypoplastic model for clays. *Computers and Geotechnics, 32*(6), 400–410.
21. Negesa, A. B. (2022). Settlement analysis of pipe culvert situated in soft clay treated with prefabricated vertical drains. *Advances in Civil Engineering*, *2022*(1), 9569077.
22. Ng, C. W. W., Hong, Y., Liu, G., & Liu, T. (2012). Ground deformations and soil-structure interaction of a multi-propped excavation in Shanghai soft clays. *Géotechnique, 62*(10), 907–921.
23. Ng, C. W. W., Wei, J., Poulos, H. G., & Liu, H. (2017). Effects of multipropped excavation on an adjacent floating pile. *Journal of Geotechnical and Geoenvironmental Engineering, 143*(7), 04017021.
24. Ng, C. W. W., Yau, T. L. Y., Li, J. H. M., & Tang, W. H. (2001). New failure load criterion for large diameter bored piles in weathered geomaterials. *Journal of Geotechnical and Geoenvironmental Engineering, 127*(6), 488–498.
25. Ong, D. E. L., Leung, C. F., & Chow, Y. K. (2006). Pile behavior due to excavation-induced soil movement in clay I: Stable wall. *Journal of Geotechnical and Geoenvironmental Engineering, 132*(1), 36–44.
26. Shakeel, M., & Ng, C. W. W. (2018). Settlement and load transfer mechanism of a pile group adjacent to a deep excavation in soft clay. *Computers and Geotechnics, 96*, 55–72.
27. Soomro, Mukhtiar Ali, and Shaokai Xiong. "Numerical Insights into Tunnel Excavation Effects on Pile-Supported Embankment in Soft Clay: A Comparison Between Consolidated and Unconsolidated Conditions." *Buildings* (2025).
28. Wang, K., Yang, Z., Guo, J., Dang, Y., & Yan, Y. (2023). Numerical analysis of the influence of deep excavation on nearby pile foundation building. *Buildings*, *13*(11), 2842.
29. Wang, L. Z., Chen, K. X., Hong, Y., & Ng, C. W. W. (2015). Effect of consolidation on responses of a single pile subjected to lateral soil movement. *Canadian Geotechnical Journal, 52*(6), 769–782.
30. Xu, J., Deng, H., Liu, Z., Dai, G., Ke, L., Guo, X., & Zhang, Z. (2025). Protection of Low-Strength Shallow-Founded Buildings Around Deep Excavation: A Case Study in the Yangtze River Soft Soil Area. *Buildings*, *15*(22), 4094.
31. Yin, Q., & Fu, H. L. (2023). Analysis of foundation pit excavation deformation and parameter influence of pile-anchor-ribbed-beam support system. *Applied Sciences*, *13*(4), 2379.
32. Zhang, R., Zhang, W., & Goh, A. T. C. (2018). Numerical investigation of pile responses caused by adjacent braced excavation in soft clays. *International Journal of Geotechnical Engineering, 10*(5), 856–864.
33. Zhang, R., Zheng, J., Pu, H., & Zhang, L. (2011). Analysis of excavation-induced responses of loaded pile foundations considering unloading effect. *Tunnelling and Underground Space Technology, 26*(2), 320–335.
34. Zhuang, X., Zong, Z., Huang, Y., Wang, C., & Lin, X. (2022). Parametric study on analyzing the effect of soil–cement strength on the uplifting behavior of HSCM piles installed in marine soft clay. *Applied Sciences*, *13*(1), 330.